NI

NASA Technical Memorandum 83182

EFFECT OF LOAD ECCENTRICITY AND SUBSTRUCTURE DEFORMATIONS ON ULTIMATE STRENGTH OF SHUTTLE ORBITER THERMAL PROTECTION SYSTEM

James Wayne Sawyer

SEPTEMBER 1981

National Aeronautics and Space Administration

Langley Research Center
Hampton, Virginia 23665

EFFECT OF LOAD ECCENTRICITY AND SUBSTRUCTURE DEFORMATIONS ON ULTIMATE STRENGTH OF SHUTTLE ORBITER THERMAL PROTECTION SYSTEMS

SUMMARY

Tension tests have been conducted at room temperature to determine the effect of load eccentricity and substructure deformations on the ultimate strength and stress-displacement properties of the Shuttle orbiter Thermal Protection System (TPS). The materials investigated are the LI-900 Reusable Surface Insulation (RSI) tiles mounted on the .41 cm (.160 inch) thick Strain Isolator Pad (SIP). The substructure deformations considered had a wavelength typical of that expected on the orbiter wing and the peak-to-peak amplitude was varied between 0 and 0.76 cm (.030 inches). Tensile loads were applied to the specimens at distances that varied between 0 and 2.54 cm (1.0 inch) from the tile center. Substructure deformations reduce the ultimate strength of the SIP/tile TPS and increase the scatter in the ultimate strength data. Substructure deformations that occur unsymmetric to the tile can cause the tile to rotate when subjected to a uniform applied load. Load eccentricity reduces SIP/tile TPS ultimate strength and causes tile rotation. A nonlinear analysis of the TPS tile system with load eccentricity and substructure deformations gives stress-displacement relationships that are in good agreement with experimental results.

INTRODUCTION

The Thermal Protection System (TPS) used for high temperature areas of the Shuttle orbiter is composed of arrays of Reusable Surface Insulation (RSI) tiles bonded to Nomex felt Strain Isolator Pads (SIP) which, in turn, are bonded to the aluminum external skin of the orbiter. The SIP and RSI are bonded using RTV-560 silicone rubber adhesive. The SIP material serves to isolate the rigid, fragile tile material from the relatively large deformations of the aluminum substructure caused by mechanical and thermal loads. The tiles, however, are subjected to a complicated set of tension/compression loads and moments as a result of the substructure deformations, aerodynamic pressures, and shocks. Thus, ultimate tensile strengths are needed for various load conditions for the full size tile/SIP system.

The results of structural tests with various combinations of tension, compression, and shear loads and applied moments are reported in references 1 and 2 for the tile/SIP systems. Test results are also presented for the tile/SIP system bonded to a curved surface to simulate substructure mismatch or initial curvature. The present investigation was undertaken to determine the combined effect of load eccentricity (bending moment) and substructure deformations on the ultimate strength of the LI-900 tile system bonded to the .41 cm (.160 inch) thick SIP. The substructure deformations considered have a wavelength typical of that expected on the orbiter wing and the amplitude is one of the test variables.

SPECIMEN DESCRIPTION

Materials

Specimens used in this investigation are made using LI-900 tiles, 0.41 cm (.160 inch) thick SIP, silicone rubber adhesive, and aluminum test fixtures. The RSI tiles are rectangular parallelepipeds, 15.2 cm (6 inch) square with a thickness of approximately 3.2 cm (1.25 inch) and a density of 144 kg/m^3 (9 lb/ft^3). The SIP is a needled (non-woven) Nomex felt and is used as a strain isolator pad between the RSI tile and the aluminum substructure. The tile is bonded to the SIP and the SIP is bonded to the test fixture using RTV-560 room temperature curing silicone rubber adhesive. The SIP was obtained from the same supply as that used for the Shuttle orbiter. Fresh adhesive was obtained from the manufacturer to insure that the shelf life had not been exceeded. The aluminum fixture surfaces that were to be bonded to the test specimens were chemically etched, sprayed with a protective primer (Koropon), and vacuum baked to remove all volatiles. The bonding procedure used to make the specimens is a very close duplicate of that used on the actual Shuttle. The bonding and quality control personnel received special training at the Kennedy Space Center to insure that the correct procedure was used in making the specimens. Care was taken to insure that the RTV adhesive had cured to a Shore hardness of 50 or greater before the specimens were tested.

Configuration

A detailed description of the test specimens used in this investigation is given in figure 1. The tile is attached to the aluminum fixture with a 12.7 by 12.7 cm (5 by 5 inch) piece of SIP and is supported around its edge by a .95 cm (.38 inch) wide strip of material called a filler bar. The filler bar is a

heat treated piece of Nomex felt which prevents hot gases flowing into the SIP. The filler bar is bonded to the aluminum fixture but not to the tile. A gap of approximately .32 cm (.13 inches) exists between the SIP and the filler bar.

The test fixture consists of a thin 25 by 25 cm (10 by 10 inches) aluminum plate riveted to five thick wall aluminum tubes. The test fixture was designed so that once the tile had been bonded to the aluminum plate and cured, the aluminum plate could be deformed to a shape typical of the substructure deformations expected on the wing region of the Shuttle orbiter. By bolting the support tubes to a rigid base plate with shims under alternative tubes (see fig. 2), the aluminum plate deforms to approximately a sine wave. The peak-to-peak wave amplitude is given by the shim thickness and the half wavelength by the 5.26 cm (2.07 inch) tube spacing.

A specimen in sequential stages of assembly is shown in figure 3a and 3b and is shown completed in figure 3c. The tile and SIP are bonded to the test fixture with the tile diagonals parallel to the edge of the test fixture as shown in figure 3c. The tile is located on the test fixture so that one corner edge of the SIP is over the centerline of one of the support tubes. An aluminum plate with a load attachment slot is bonded to the top of the tile to provide a variable load attachment point. The attachment point can be located up to $\pm$2.5 cm (1.0 inch) from the center of the tile along a tile diagonal perpendicular to the support tubes.

TEST DESCRIPTION

Proof Tests

A proof test was conducted on each specimen prior to its acceptance for structural testing in accordance with techniques approved for testing TPS on the Shuttle orbiter. The test involved applying transverse tension and com-

pression loads to the TPS sufficient to impose an average stress on the SIP of 55.2 kPa (8 psi). The load was applied and removed at the rate of 13.8 kPa/sec (2 psi/sec) stress on the SIP. The tension load was held for 30 seconds at the 34.5 kPa (5 psi), 41.4 kPa (6 psi), 48.3 kPa (7 psi) stress levels and for 60 seconds at the 55.2 kPa (8 psi) stress level. The compression load was held for 30 seconds at the 55.2 kPa (8 psi) stress level. Acoustic emission data was monitored and recorded during the proof test. The acoustic test equipment was calibrated using a standard gage that had characteristics almost identical to the standard used at Kennedy Space Center.

TPS specimens were accepted for structural testing if the acoustic counts during the proof test did not exceed any of the following conditions:

1. 250 counts during the first 30 seconds of the 60-second constant proof load.
2. 100 counts during the second 30 seconds of the 60-second constant proof load and less than the number of recorded counts during the first 30 seconds when counts exceed 50 for either the first or second 30-second period.
3. 2000 counts from start of test at zero load to the midpoint of constant proof load interval.

Following the proof test, each tile was wiped with alcohol and examined to identify any cracks in the tile coating. Specimens failing the proof test were rejected.

A photograph of the proof test setup is shown in figure 4, and a typical proof stress-displacement curve is shown in figure 5. A pneumatic jack was used to apply the load and an automatic pressure regulator system imposed the pre-programmed load/time profile. Acoustic emission transducers were located at the four sides of the tile. A load cell measured the force applied to the tile. Acoustic emission data, loads, and displacements were recorded during the test.

Tension Test

The tension tests were conducted in a controlled displacement test machine at a displacement rate of 0.13 cm/min (.05 inches/min). A 2.2 kN (500 lbs) tension load cell was used to measure the applied load. The tile displacement was measured using four displacement gages stationed at the midsurface of each tile edge. The displacement measurements were made between the top plate of the tile and the aluminum plate substructure. A photograph of the test setup is shown in figure 6.

The tile test assembly was mounted on a base plate with shims installed under alternate support tubes (see figure 2) to give the desired substructure deformation. The tile base plate assembly was then clamped to the moveable crosshead of the test machine so that the center of the tile was aligned with the axis of the test machine. The top of the tile was attached to the stationary crosshead of the machine through a load cell and a spherical swivel. The swivel was attached off-center to the tile to give the desired eccentric loading. The eccentricity, e, and the substructure peak-to-peak deformation amplitude, s, for each test is given in table I.

Load and displacement data were recorded using x-y recorders. Before installing the tile assembly in the test machine, the load cell output was zeroed. After attaching the load cell to the tile, the crosshead was moved until the load cell output indicated zero load. The x-y recorders were then zeroed and the specimens were tested to failure with a tensile load. Care was exercised in installing the tile test assembly to minimize setup loads.

RESULTS AND DISCUSSION

Tension Tests

A total of 24 TPS tile specimens were tested during this investigation. Typical stress-displacement results are shown in figures 7 through 10 for specimens with and without load eccentricity and substructure deformations. Curves are given for the displacement of the midpoint of each of the edges of the tiles (see sketches in figures 7 through 10). For specimens with no substructure deformation and no load eccentricity (see figure 7), average stress-displacement curves for the tile are given by the dashed line. For specimens with substructure deformations or load eccentricity, stations 1 and 4 are located at identical points relative to the substructure waveform and the load. Stations 2 and 3 are also at identical points relative to the substructure waveform and load but are at a different position from stations 1 and 4. Thus in figures 8 through 10, average stress-displacement curves are given for stations 1 and 4 and stations 2 and 3 by the dashed lines.

For specimen number 2 with no substructure deformation and no load eccentricity (see figure 7), the stress-displacement curves show nonlinear behavior typical of the SIP material, that increases in stiffness with increase in stress level. The differences in displacements at the midpoints of the tile edges are due to the non-uniformity of the SIP material and possible slight misalignment of the load attachment. Stress-displacement curves are given in figure 8 for specimen number 9 with the substructure deformed into a sine wave with an amplitude of .076 cm (.030 inches) and a wavelength of 10.5 cm (4.14 inches). The stress-displacement curves at stations 1 and 4 (see sketch in figure 8) are similar to stations 2 and 3 but have less displacements for a given load. The differences in the stress displacement curves at stations 1

and 4 and stations 2 and 3 indicate that substructure deformations cause some tile rotation even with the specimen loaded through its centroid. The tile rotations depend on the location of the tile relative to the substructure waveform and would be expected to be close to zero if the center of the tile were located symmetric to the waveform. However, small rotations may be obtained due to the nonuniformity of the SIP material as was shown in figure 7.

Stress-displacement curves for typical TPS specimens with the load applied 2.54 cm (1.0 inches) from the center of the tile are shown for a tile with and without substructure deformations in figures 9 and 10, respectively. The eccentric loading results in relatively large tile rotations as indicated by the stress-displacement curves for the tile edges. The edges of the tile opposite the applied load (stations 1 and 4) show very little deflections, whereas, the edges of the tile near the applied load (stations 2 and 3) experiences relatively large deflections (.08 cm (.03 inches)) even for small (less than 14 kPa (2 psi)) average applied stress levels. Comparison of figures 9 and 10 indicate that for eccentrically loaded tiles, a sine wave substructure deformation amplitude of .076 cm (.030 inches) does not significantly increase the tile rotation or change the stress-displacement relationship for the tile system.

Two to four replicate tests were made for each load eccentricity and substructure deformation amplitude. Average stress-displacement curves of replicate tests are shown in figures 11 through 14. The stress-displacement curves presented in figures 11 and 12 are for specimens with the load applied through the tile center and in figures 13 and 14 for the load applied 2.54 cm (1.0 inches) from the tile center. The data presented in figures 11 and 13 are for a tile with no substructure deformation and the data in figures 12 and 14 are for a tile with a substructure wave amplitude of .076 cm (.030 inches).

Two stress-deflection curves are given for the specimens with substructure deformations or with the load applied eccentric to the center of the tile. The two curves are an average of the deflections at the midpoint of the tile edges toward (Location A) and away (Location B) from the applied load. The differences in the stress-displacement curves for the duplicate tests are large and indicate there are large variations in the material properties of the TPS system. Thus, a large number of tests are required to determine the bounds of the material properties and to obtain useful design data.

Average stress-displacement curves for TPS tiles with and without loading eccentricity are shown in figure 15. The curves shown are an average of the displacements measured at stations 2 and 3 for all specimens tested. The results show that load eccentricity has a predominant effect on the stress-displacement relationship, whereas, substructure deformations have only a minor effect. The eccentric loading causes tile rotations which would result in steps in the tile surface on the vehicle. If tile rotations occur so that forward facing steps are formed, the resulting aerodynamic loading tends to increase the load eccentricity and thus the tile rotation. Rearward facing steps, although undesirable, would be reduced by the resulting aerodynamic loading.

Analysis

The nonlinear analysis presented in reference 3 was used to calculate stress-displacement curves for comparison with the experimental results. The analysis assumes that the tile is rigid and that the SIP and filler bar behave as nonlinear spring foundations where the spring response characteristics are obtained using experimental stress-strain data. The effects of combined loads and moments are included. An unpublished experimental edge-effect study,

conducted by Philip Ransone and Donald Rummler of the Materials Division, Langley Research Center, has shown that the SIP has a lower stiffness near an edge. Thus, the lower stiffness charateristics of the SIP edges was taken into account in the analysis using a two-strip approximation to the edge stiffness developed from the experimental study. The two-strip method consists of dividing the SIP into a large center square surrounded by two strips each .64 cm (.25 inches) wide. The stiffness of the inner and outer strips of SIP are reduced by 25 and 50 percent, respectively. These strip widths and stiffness reductions were determined by Wolf Elber of the Materials Division, Langley Research Center, to show good agreement with the edge effect study. The stress-strain data used in the analysis were obtained from the tile results presented in figure 7.

The calculated stress-displacement curves are shown by the dashed lines in figures 12 through 14. In general, the calculated and experimental stress-displacement curves are in good agreement with most of the calculated curves falling within the experimental data scatter. The largest deviation of calculated results from experiment was obtained for the specimen with a .076 cm (.030 inch) substructure wave amplitude and with the load applied through the center of the tile (see figure 12). The analysis did not show as large an effect of substructure deformations on tile rotation as was obtained experimentally. However, the analysis did accurately account for the tile rotation due to the eccentric loading (see figures 13 and 14).

Ultimate Strength

Each of the TPS tile specimens were loaded to failure to obtain their ultimate strength. The ultimate load for each specimen is given in table I along with the load eccentricity and substructure deformation. Most specimen

failures occurred at the SIP/tile interface similar to results reported in references 1 and 2. However, as noted in table I, four specimens failed in the tile near the top plate. These four tile failures occurred at loads as high or higher than SIP/tile interface failures for similar specimens with the same load eccentricities and substructure deformations. The tile failures are thought to be due to propagation of cracks that existed in the tile before the tests. Large variations in ultimate loads are obtained for replicate tests as were observed in references 1 and 2. Although a large number of specimens would have to be tested to give statistically valid ultimate loads, the limited test results can be used to show trends. Average ultimate loads for all replicate specimens are shown in table II for each load eccentricity and substructure deformation. The average values shown include the four tests that had tile failures.

The effect of load eccentricity and substructure deformations on ultimate strength is shown in figure 16 where the ultimate load is shown as a function of the substructure deformations. Data are shown for the load applied at an eccentricity of 0, 1.25, and 2.54 cm (0, .5 and 1.0 inches). The dashed lines are faired through the average of the test data. In general, substructure deformations reduce the ultimate strength of the TPS. For example, with the force applied through the center of the tile, a specimen with a substructure deformation amplitude of .076 cm (.030 inches) has approximately a 20 percent lower ultimate strength than a specimen with a undeformed substructure. Also, increasing the substructure deformation amplitude significantly increases the data scatter for the small number of specimens tested. An exception to the reduced ultimate strength due to substructure deformations can be seen for the largest eccentricity of 2.54 cm (1.0 inches) where a substructure deformation amplitude of .038 cm (.015 inches) has slightly higher ultimate strength than

a tile with a larger or smaller amplitude substructure deformation. However, the slightly higher ultimate strength values are insignificant in view of the data scatter and the small number of specimen tests.

Load eccentricity also has a detrimental effect on the maximum load carrying ability of the TPS. For example, specimens with an eccentricity of 2.54 cm (1.0 inch) have ultimate tensile loads 35 to 40 percent less than that of specimens with the load applied through the center of the tile either with or without substructure deformations.

CONCLUDING REMARKS

Tension tests have been conducted at room temperature to determine the effect of load eccentricity and substructure deformations on the ultimate strength and stress-displacement properties of the Shuttle orbiter TPS system. The materials investigated are the LI-900 RSI tiles mounted on the .41 cm (.160 inch) thick SIP. The substructure deformations considered had a wavelength typical of that expected on the orbiter wing and the peak-to-peak amplitude was varied between 0 and .076 cm (.030 inches). Combined tension and moment loads were applied to the specimens by varying the location of applied load from 0 to 2.54 cm (1.0 inch) from the tile center.

The test results show that substructure deformations reduce the ultimate strength of the SIP/tile TPS and increase the scatter of the specimen failure load A uniform applied tension load to the top of a tile can cause tile rotation about an inplane axis if the substructure is deformed asymmetrically with respect to the center of the tile planform. Load eccentricity reduces the maximum tensile load the SIP/tile TPS can carry. Nonlinear analysis of the TPS tile system with load eccentricity and substructure deformations give stress-displacement relationships that are in good agreement with experimental results.

REFERENCES

1. Williams, Jerry G.: Structural Tests of a Tile/Strain Isolation Pad Thermal Protection System. NASA TM-80226, March 1980.

2. Williams, Jerry G.: Structural Tests on Space Shuttle Thermal Protection System Constructed with Nondensified and Densified LI-900 and LI-2200 Tile. NASA TM-81903, January 1981.

3. Housner, Jerrold M.; and Garcia, Ramon: Nonlinear Static TPS Analysis. NASA TM-81785, March 1980.

TABLE I - TEST CONDITIONS AND RESULTS

SPECIMEN NO.	ECCENTRICITY, e		PEAK-TO-PEAK SUBSTRUCTURE DEFORMATION, δ		ULTIMATE STRENGTH	
	CM	INCHES	CM	INCHES	kN	LBS
1	0	0	0	0	1.51	340
2	0	0	0	0	1.41	316
3	0	0	0	0	1.49*	336
4	0	0	0	0	1.33	300
5	0	0	.038	.015	1.41*	316
6	0	0	.038	.015	1.25*	280
7	0	0	.076	.030	1.21	272
8	0	0	.076	.030	.93	210
9	0	0	.076	.030	1.37*	308
10	1.27	0.5	0	0	1.38	310
11	1.27	0.5	0	0	1.26	284
12	1.27	0.5	.038	.015	1.14	256
13	1.27	0.5	.038	.015	1.30	292
14	1.27	0.5	.038	.015	1.16	260
15	1.27	0.5	.076	.030	1.01	228
16	1.27	0.5	.076	.030	.85	190
17	2.54	1.0	0	0	.82	185
18	2.54	1.0	0	0	.85	192
19	2.54	1.0	0	0	.85	192
20	2.54	1.0	.038	.015	.85	190
21	2.54	1.0	.038	.015	.91	204
22	2.54	1.0	.076	.030	.54	122
23	2.54	1.0	.076	.030	.79	178
24	2.54	1.0	.076	.030	.91	204

* Failure occurred in tile near top plate.

TABLE II. - AVERAGE FAILURE LOADS

NUMBER OF SPECIMENS	ECCENTRICITY, e		PEAK-TO-PEAK SUBSTRUCTURE DEFORMATION, δ		AVERAGE ULTIMATE STRENGTH	
	cm	inches	cm	inches	kN	lbs.
4	0	0	0	0	1.47	323
2	0	0	0.038	0.015	1.35	298
3	0	0	0.076	0.030	1.19	263
2	1.27	0.5	0	0	1.35	297
3	1.27	0.5	0.038	0.015	1.22	269
2	1.27	0.5	0.076	0.030	0.94	209
3	2.54	1.0	0	0	0.85	190
2	2.54	1.0	0.038	0.015	0.89	197
3	2.54	1.0	0.076	0.030	0.76	168

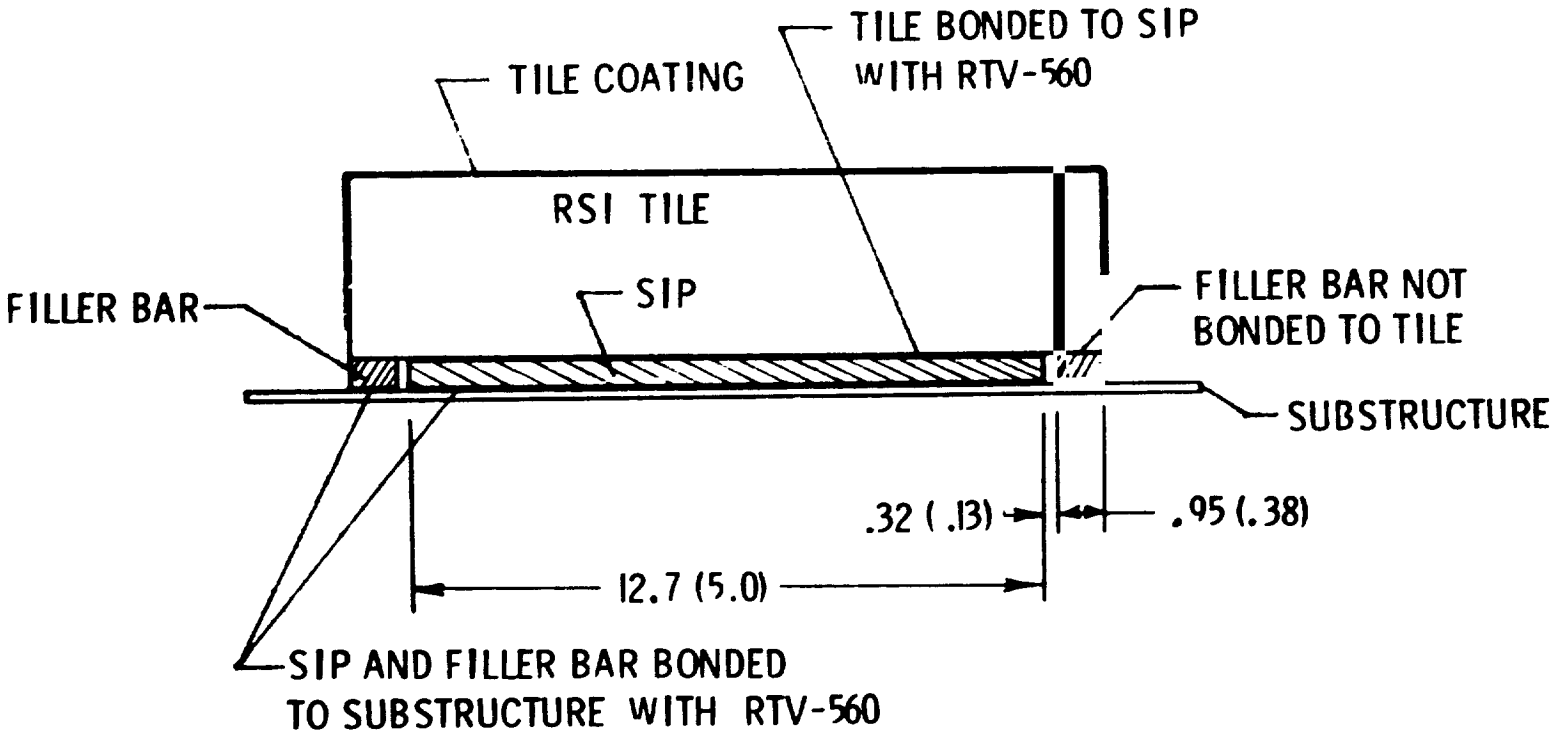

Figure 1.- Description of TPS system. Dimensions are in centimeters (inches).

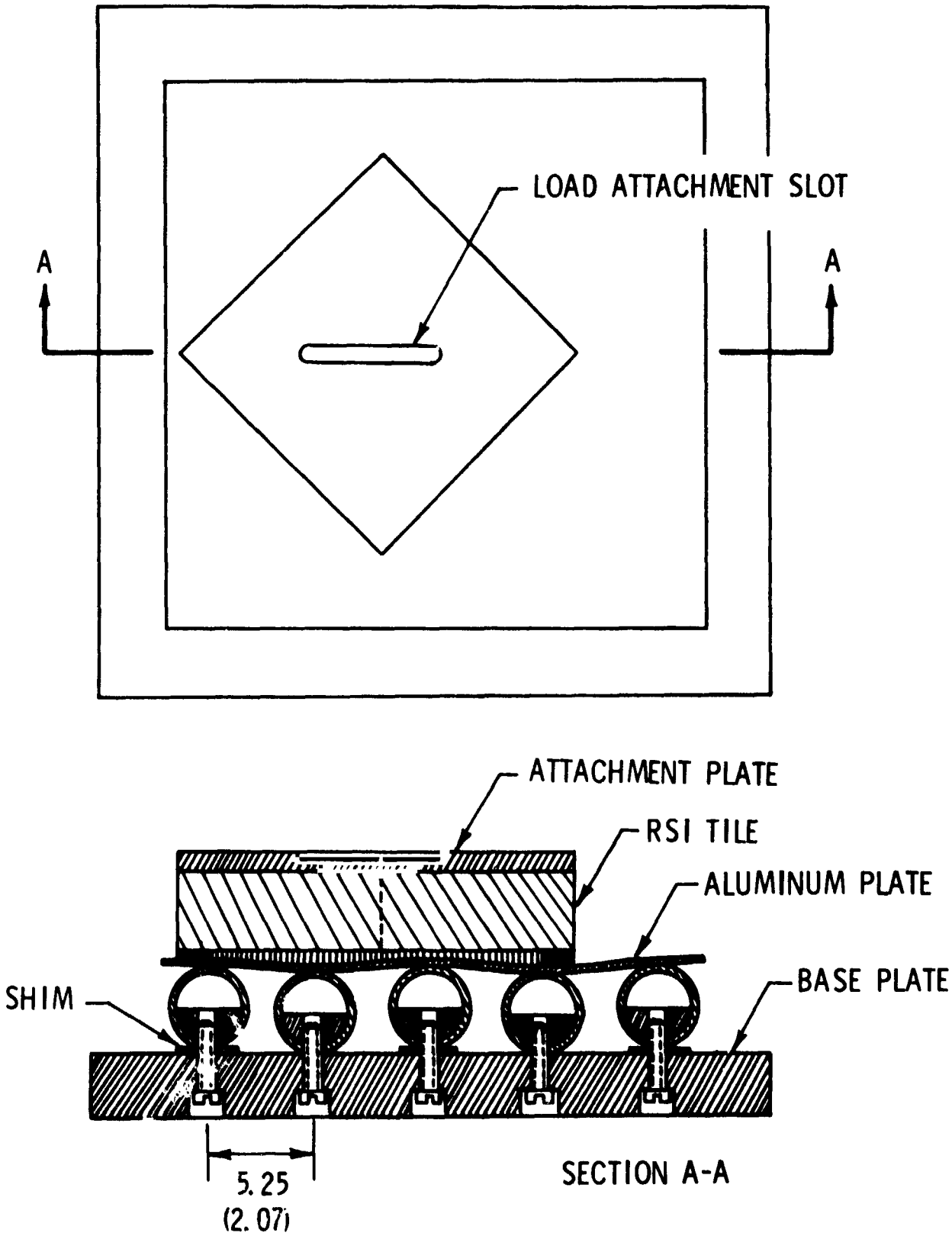

Figure 2.- TPS test specimen and test fixture. Dimensions are in centimeters (inches).

(a) Specimen parts

Figure 3.- Photograph illustrating sequential stages of specimen assembly.

(b) Partial assembly

Figure 3- Continued.

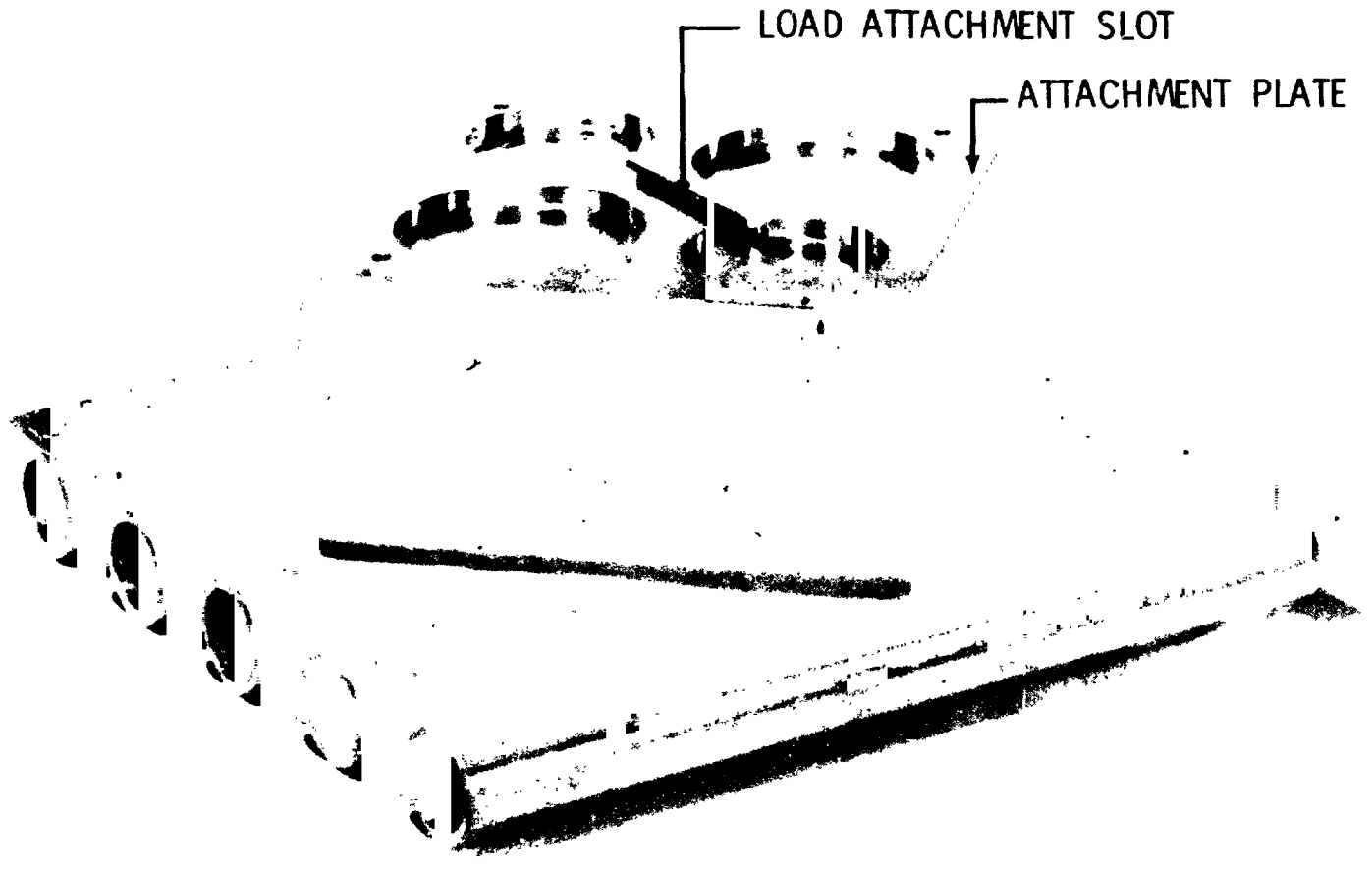

(c) Completed specimen

Figure 3- Concluded.

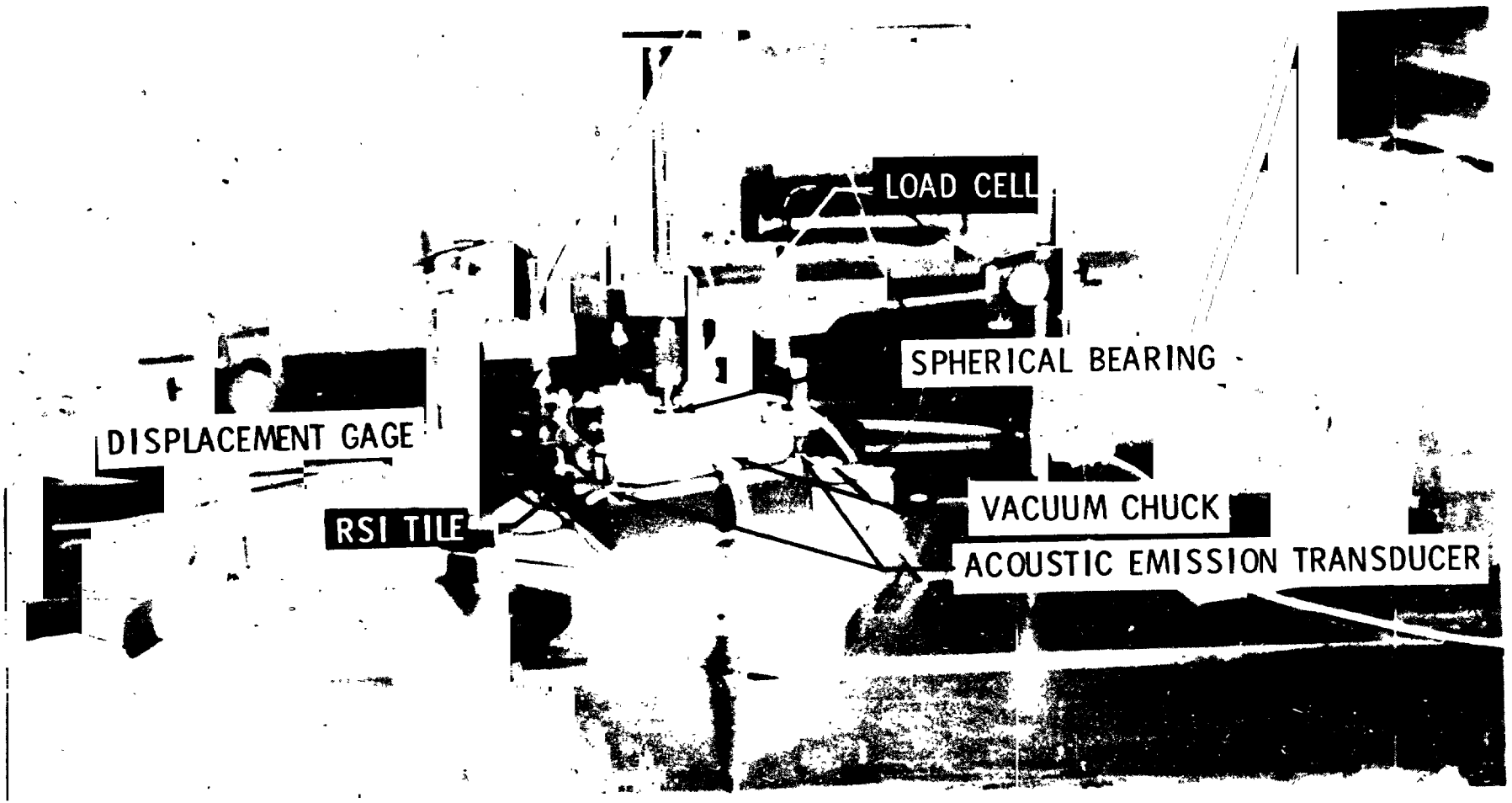

Figure 4.- Photograph of TPS specimen and proof test apparatus.

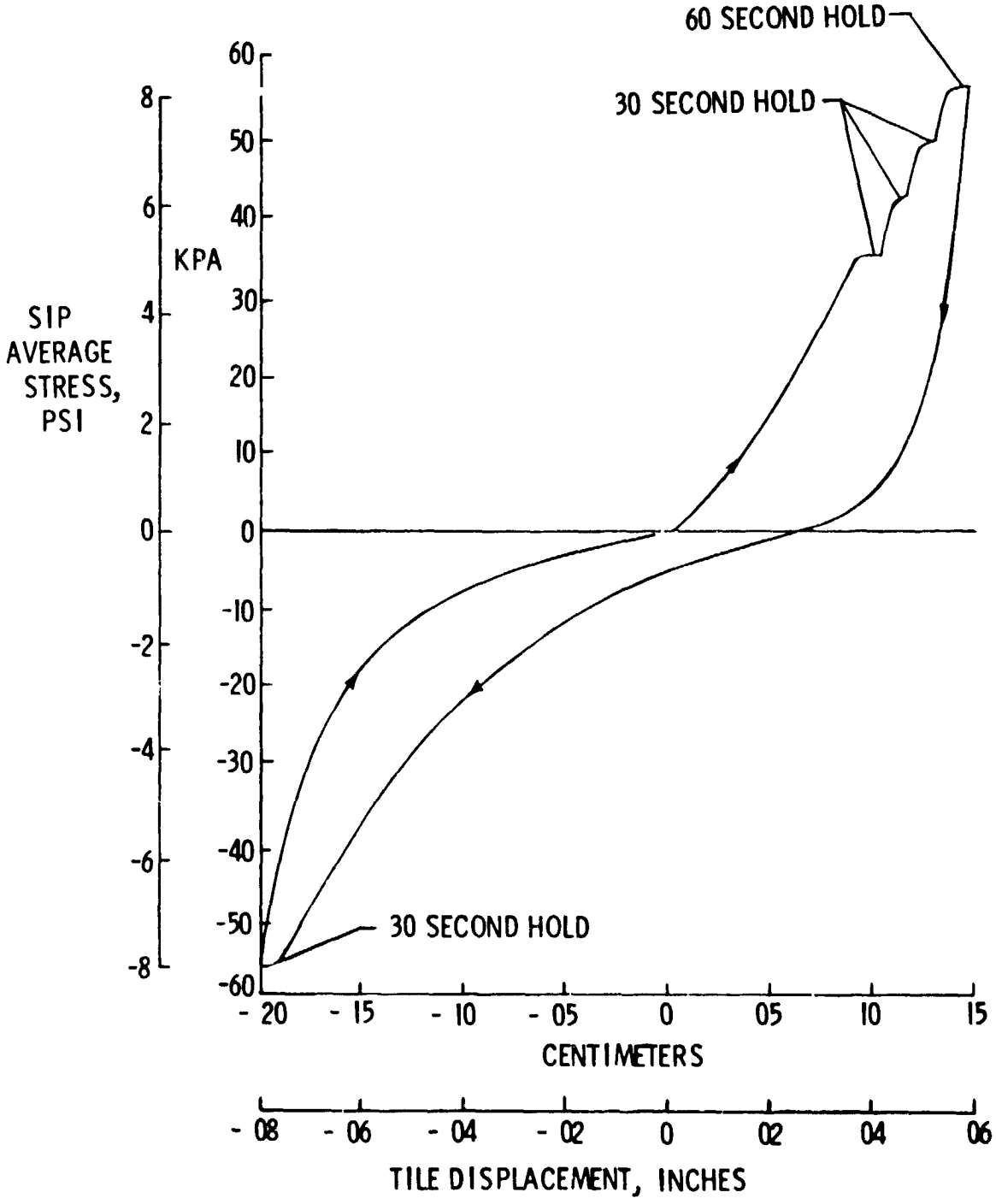

Figure 5.- Typical stress-displacement relationship for proof test of TPS specimen.

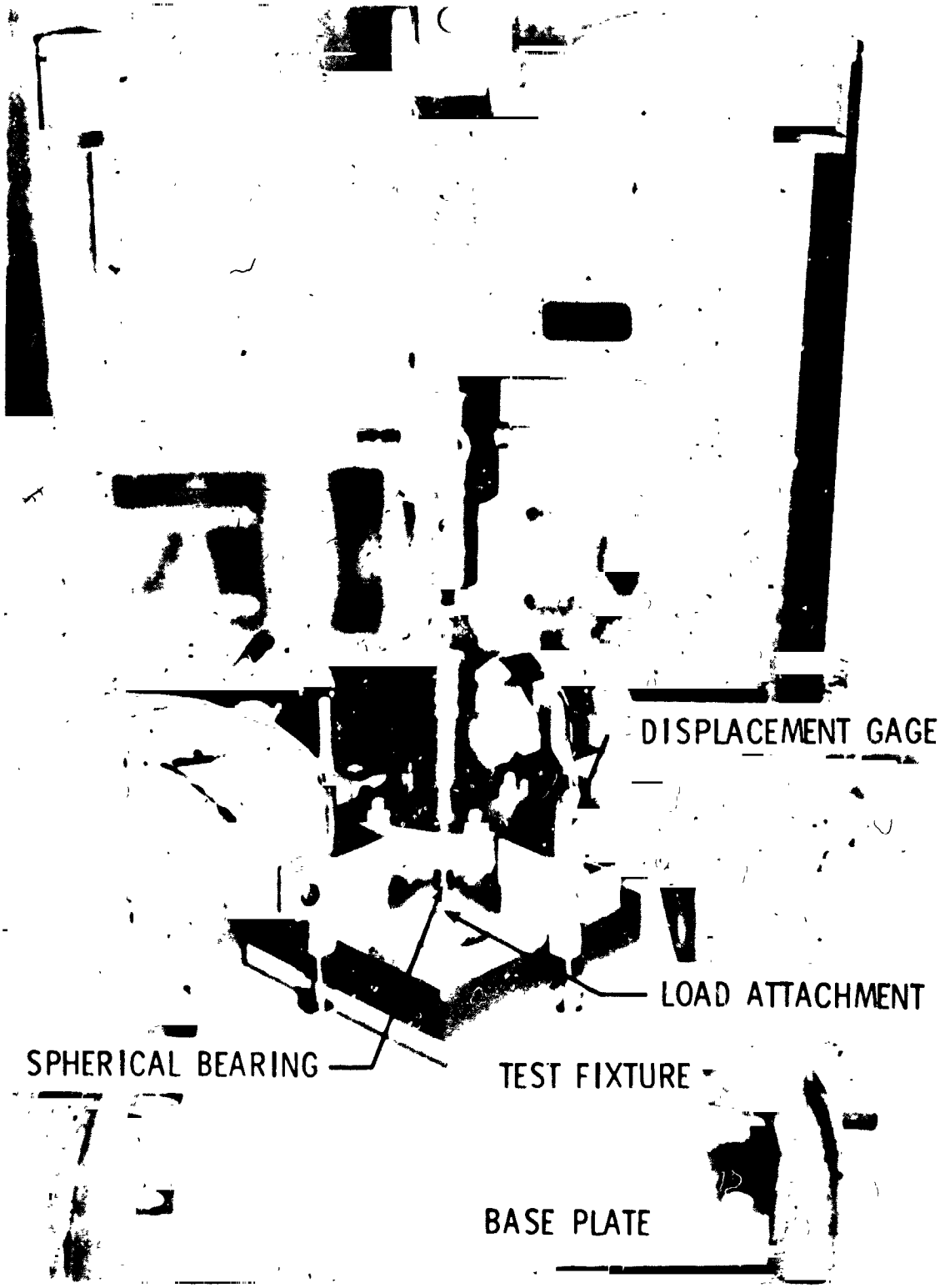

Figure 6.- Photograph of TPS specimen in test machine.

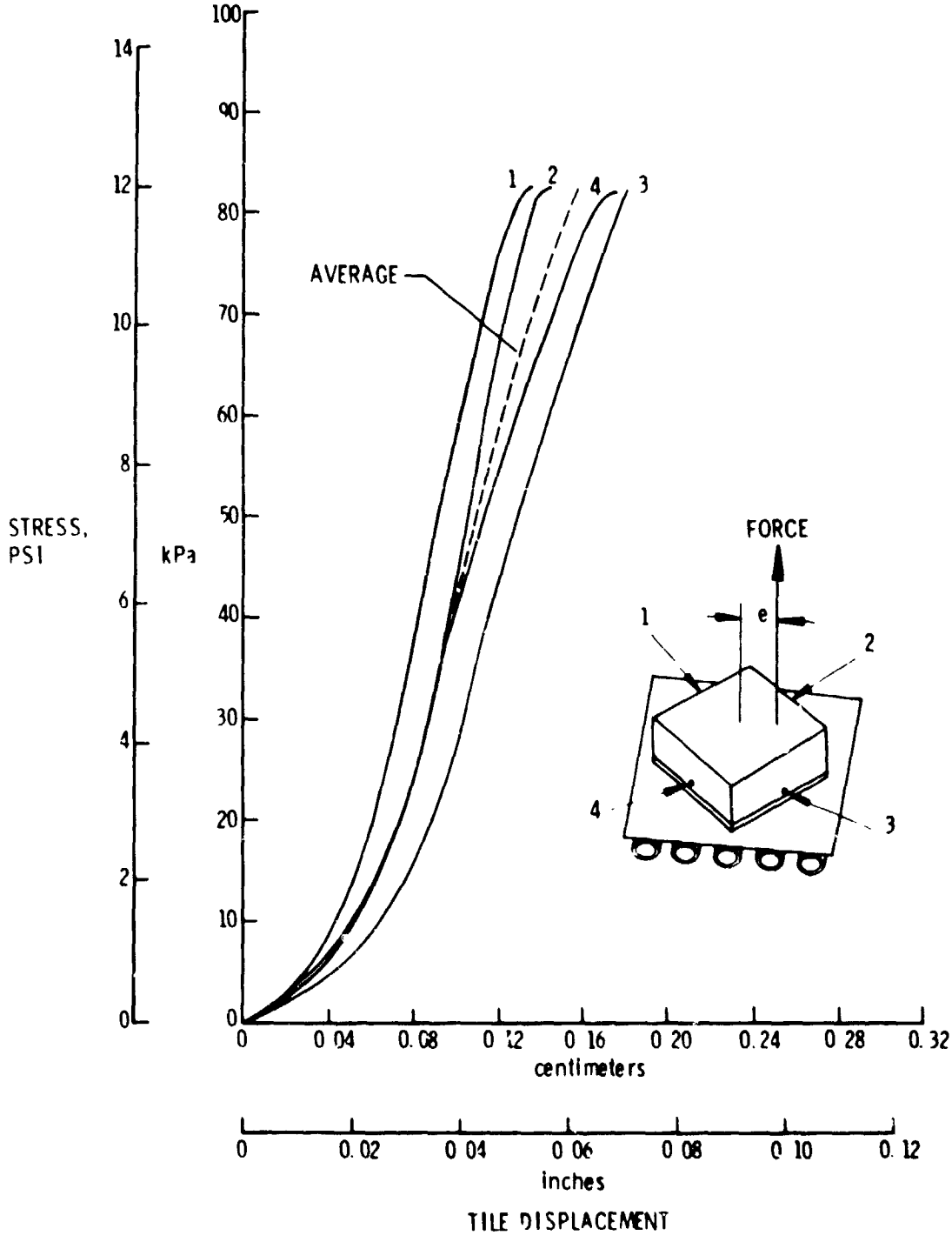

Figure 7.- Typical stress-displacement curves for TPS tile with no substructure deformation and the load applied through center of tile.

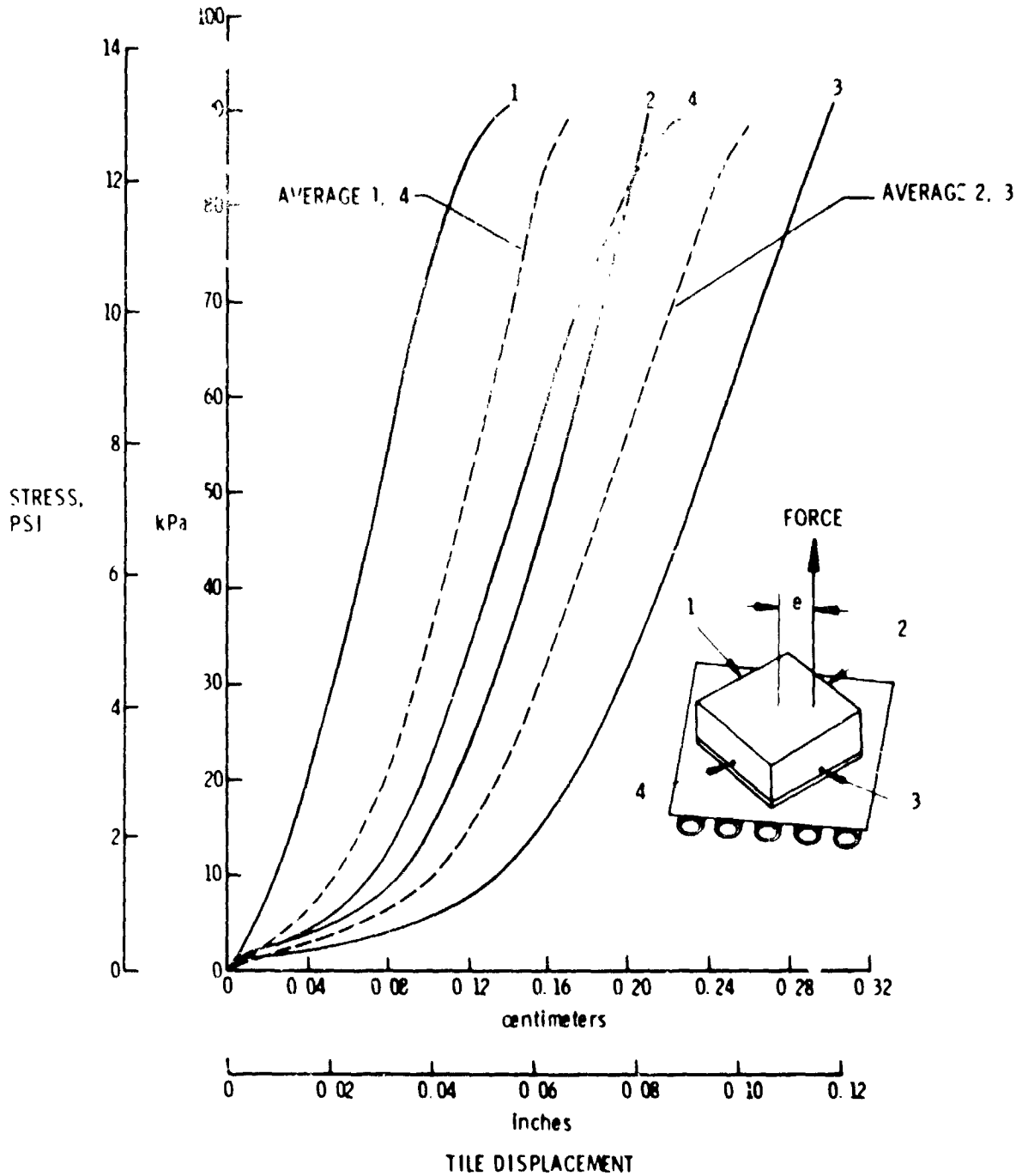

Figure 8.- Typical stress-displacement curves for TPS tile with a peak-to-peak substructure deformation of .076 cm (.030 inches) and with the load applied through center of tile.

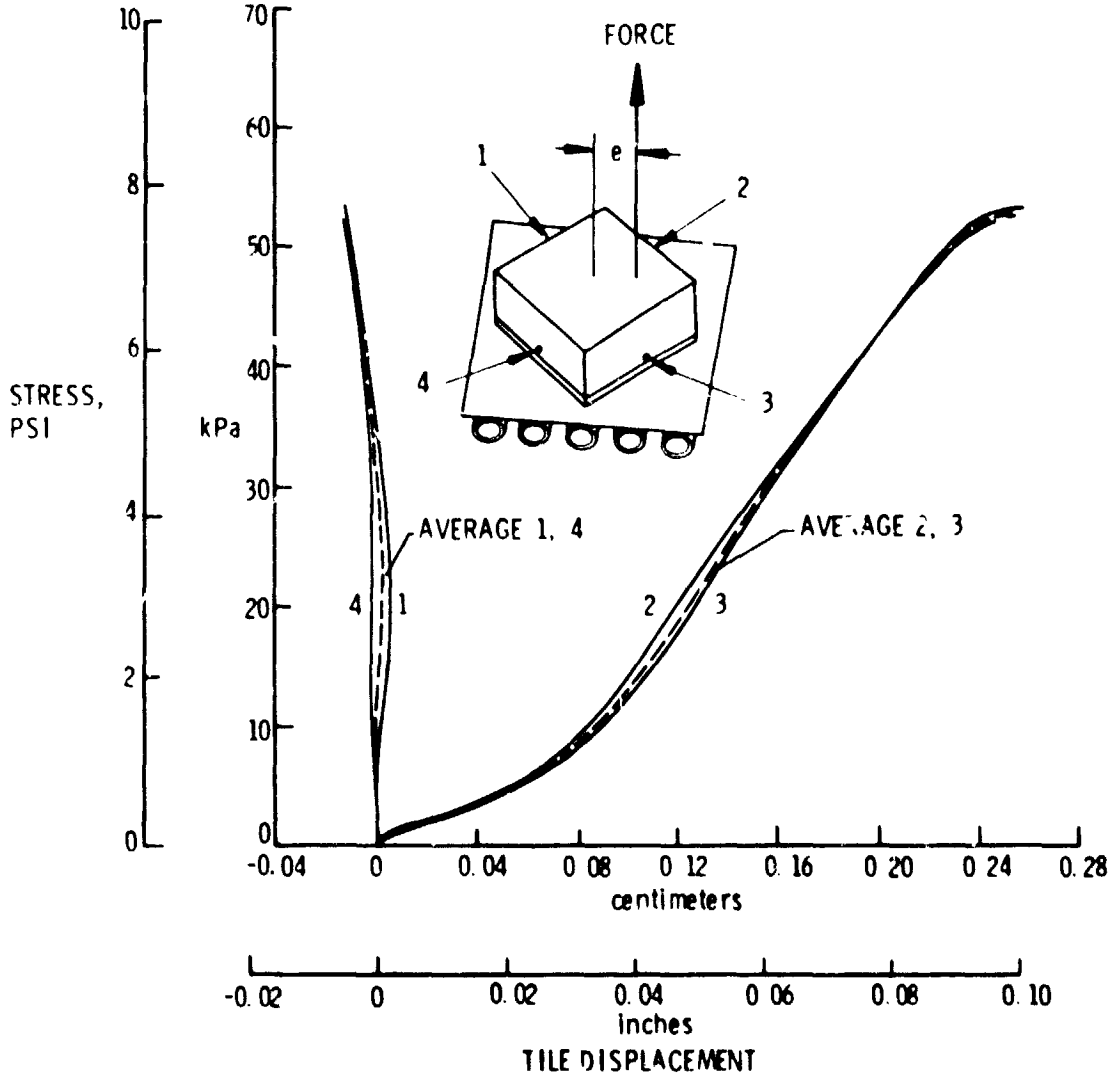

Figure 9.- Typical stress-displacement curves for TPS tile with no substructure deformation and with the load applied at an eccentricity (e) of 2.54 cm (1.00 inch) from the center of the tile.

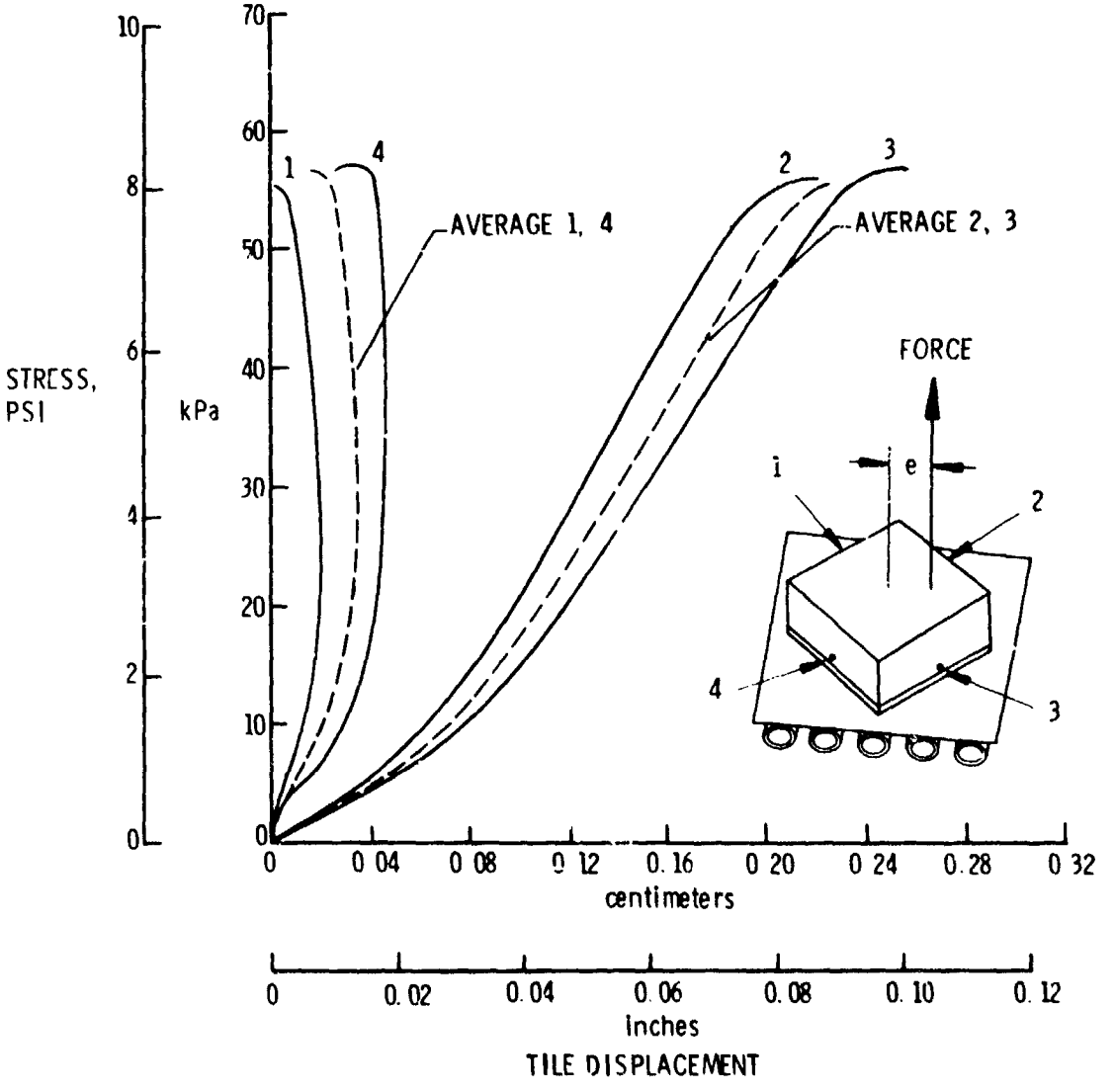

Figure 10.- Typical stress-displacement curves for TPS tile with peak-to-peak substructure deformation of .076 cm (.030 inches) and with the load applied at an eccentricity (e) of 2.54 cm (1.00 inches) from the center of the tile.

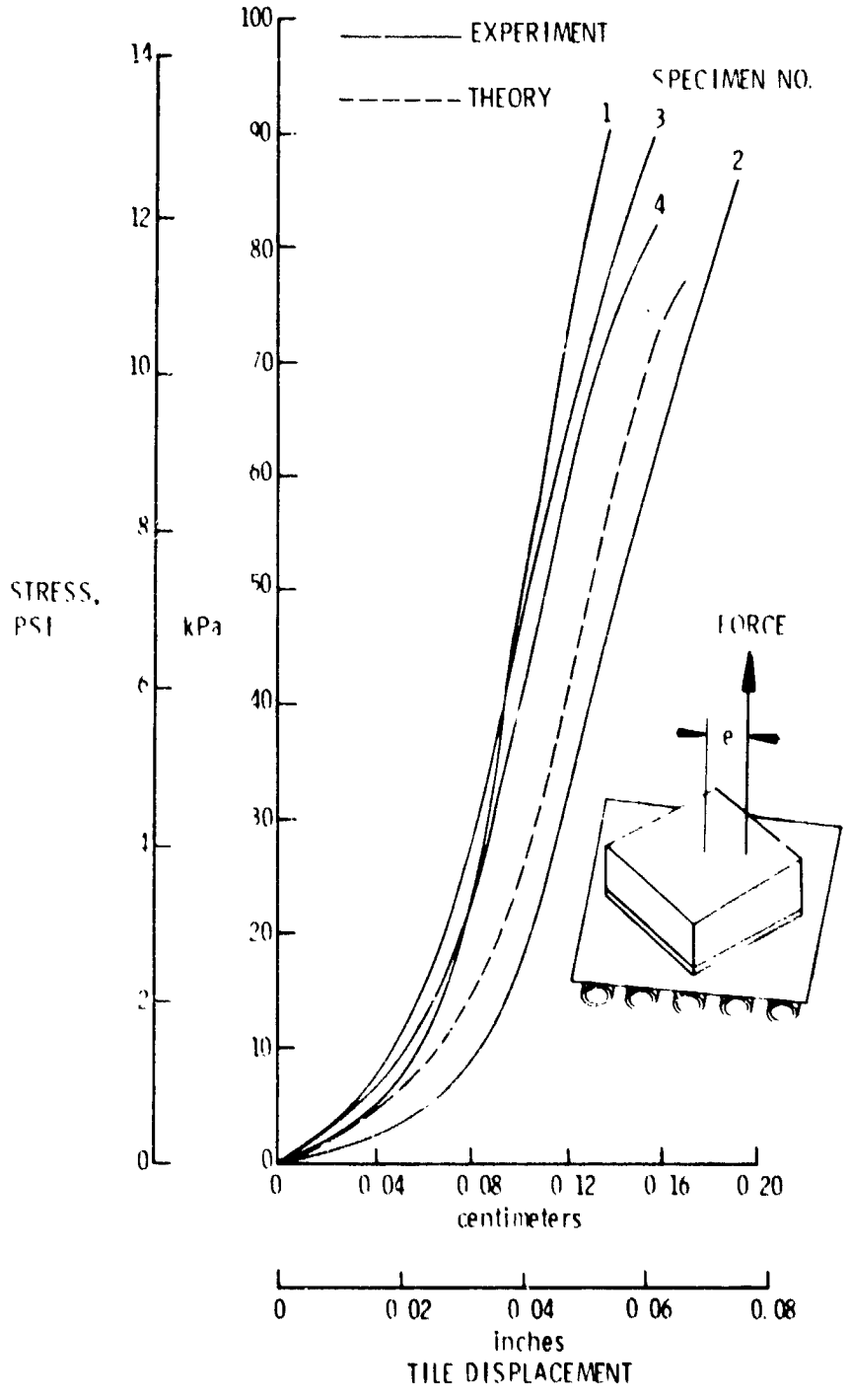

Figure 11.- Variations in average stress-displacement curves for TPS tiles with no substructure deformations and the load applied through center of tile.

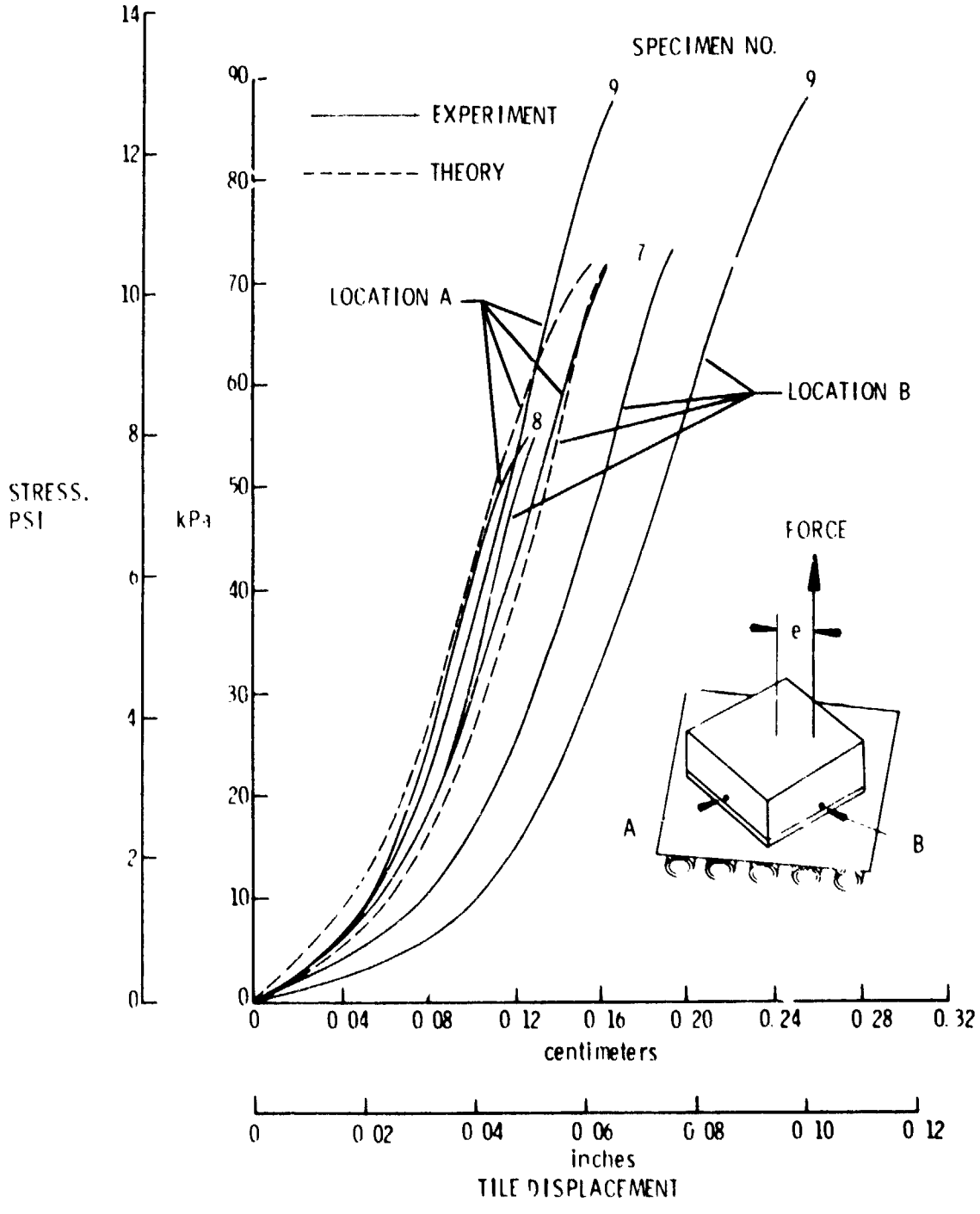

Figure 12.- Variations in average stress-displacement curves for TPS tiles with peak-to-peak substructure deformation of .076 cm (.030 inches) and with the load applied through center of tile.

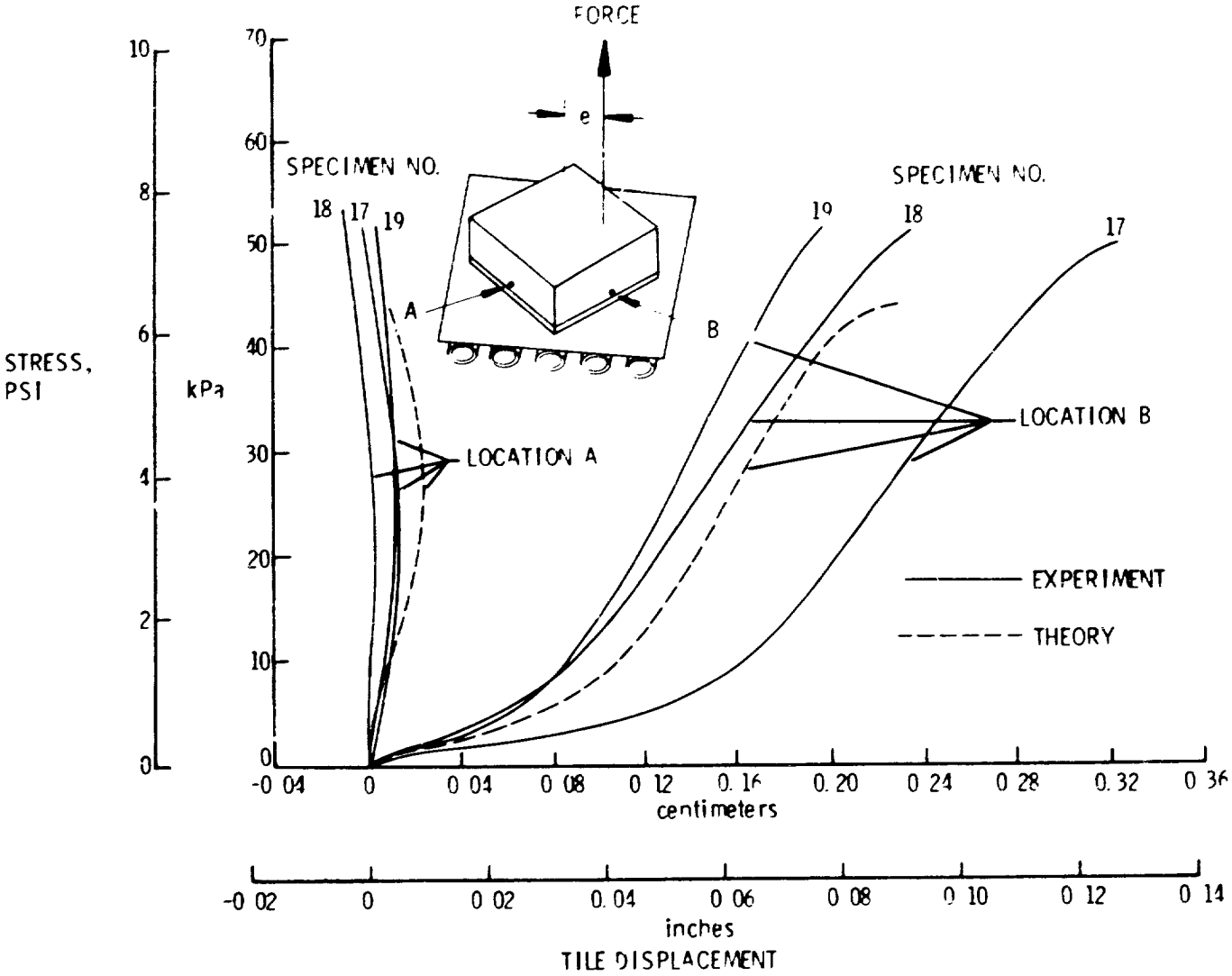

Figure 13.- Variations in average stress-displacement curves for TPS tiles with no substructure deformation and with the load applied at an eccentricity (e) of 2.54 cm (1.00 inches) from the center of the tile.

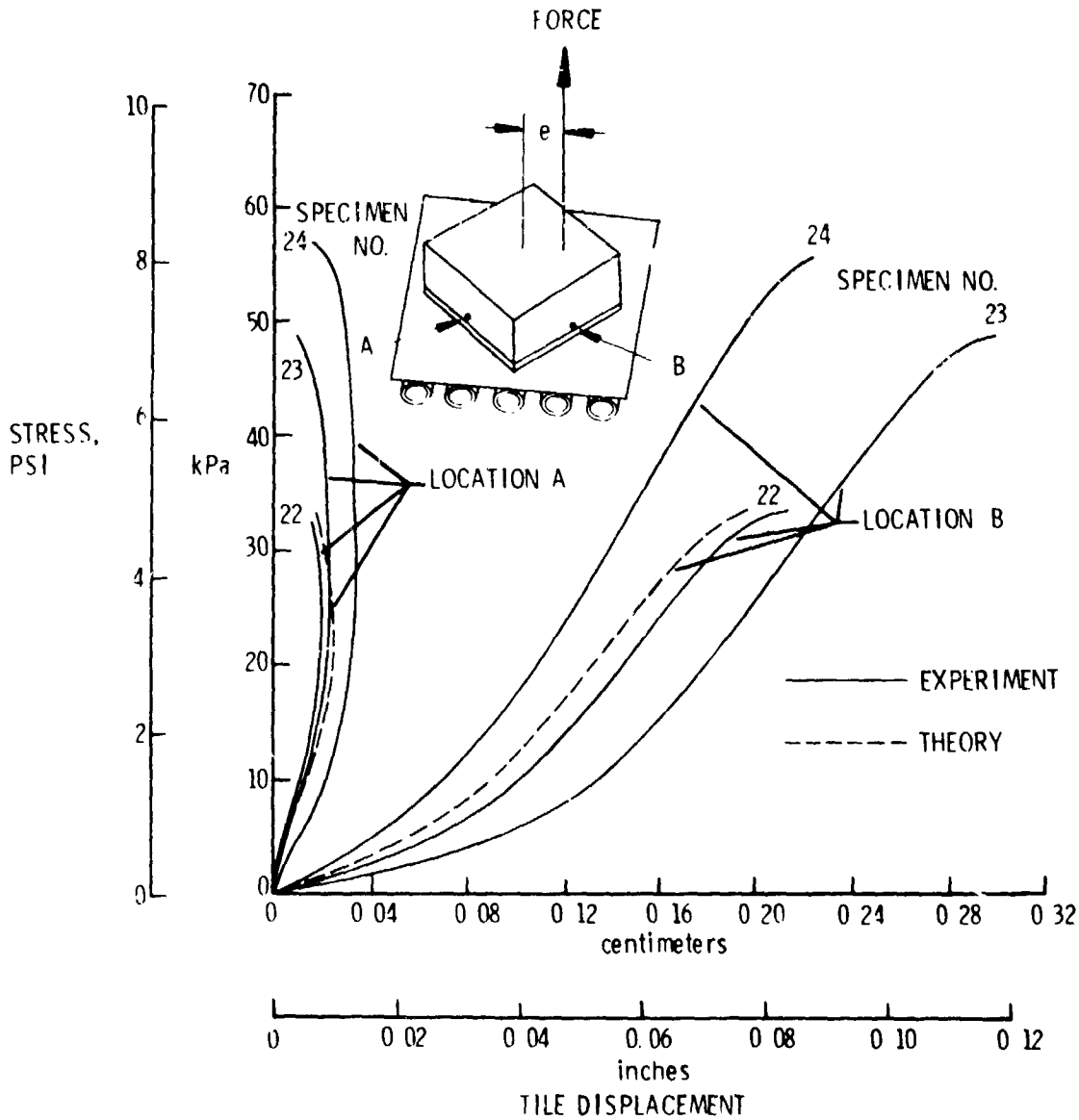

Figure 14.- Variations in average stress-displacement curves for TPS tiles with peak-to-peak substructure deformation of .076 cm (.030 inches) and with the load applied at an eccentricity (e) of 2.54 cm (1.00 inches) from the center of the tile.

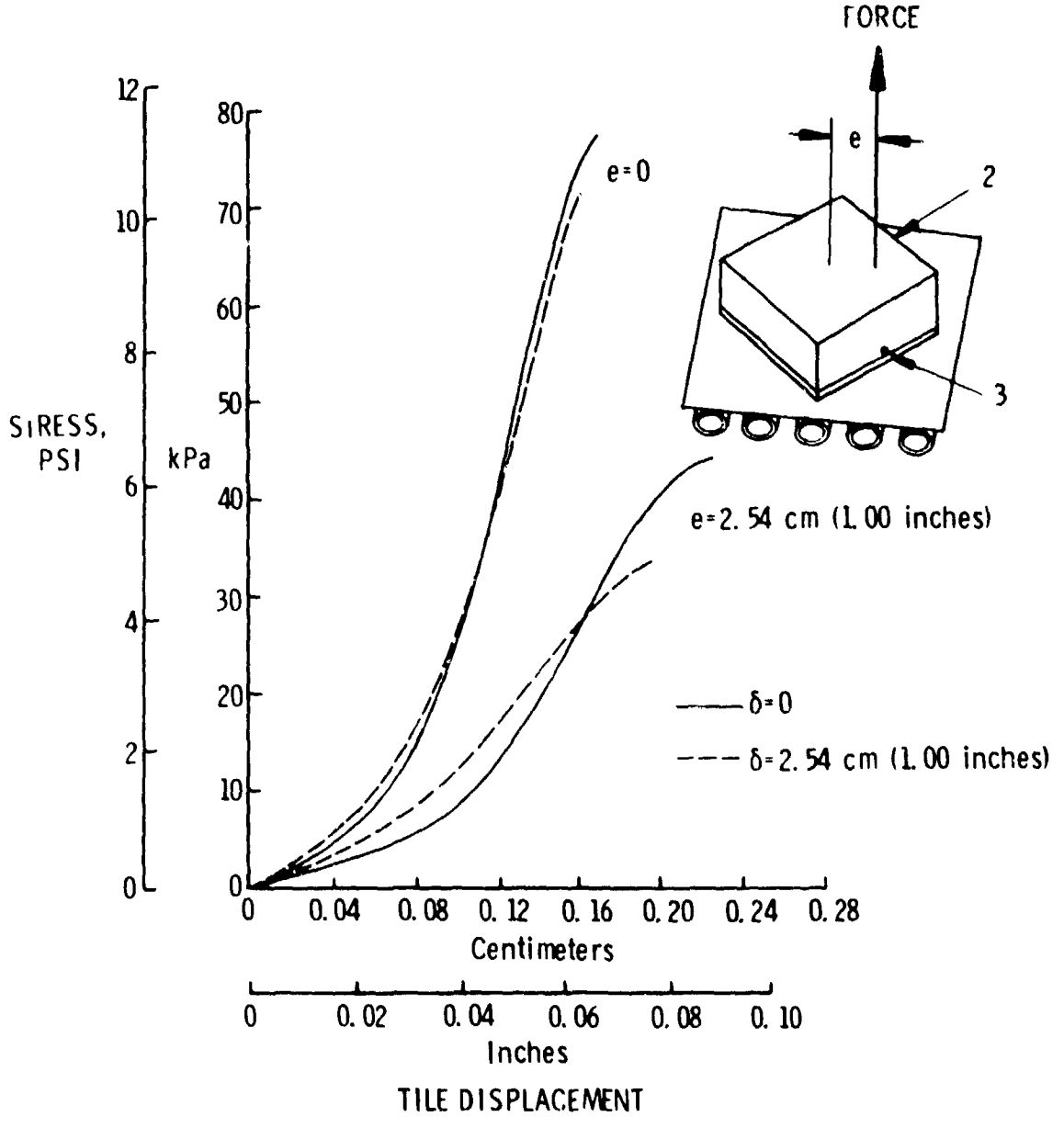

Figure 15 - Effect of substructure deformation and load eccentricity on average stress-displacement curves for TPS.

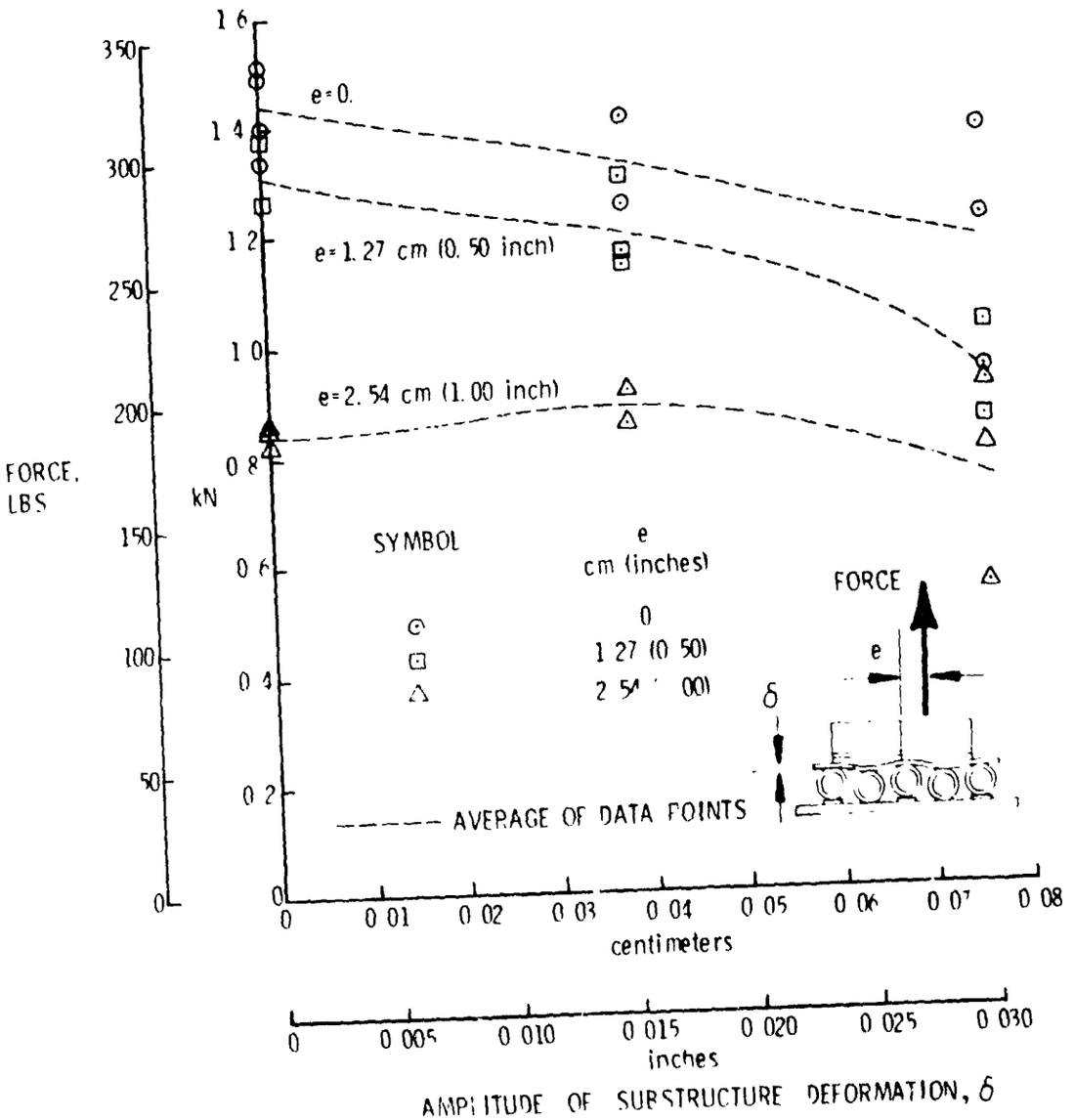

Figure 16 - Effect of load eccentricity and substructure deformation on ultimate strength of TPS tile system.